IEEE Access
Multidisciplinary : Rapid Review : Open Access Journal

Received August 8, 2019, accepted August 17, 2019, date of publication August 21, 2019, date of current version September 5, 2019.

Digital Object Identifier 10.1109/ACCESS.2019.2936554

Crack Monitoring for Hot-Spot Areas Under Time-Varying Load Condition Based on FCM Clustering Algorithm

HU SUN, JUNYAN YI, YU XU, YISHOU WANG, AND XINLIN QING
School of Aerospace Engineering, Xiamen University, Xiamen 361005, China

Corresponding authors: Hu Sun (sunhu@xmu.edu.cn) and Xinlin Qing (xinlinqing@xmu.edu.cn)

This work was supported in part by the National Natural Science Foundation of China under Grant 11902280 and Grant 11972314, and in part by the Natural Science Foundation of Fujian Province under Grant 2018J05094.

ABSTRACT Crack monitoring for damage-prone structural area, named hot-spot, is one of the most interesting concerned technologies for aircraft structural health monitoring. This paper proposes an efficient technique based on Fuzzy c-means (FCM) clustering algorithm to monitor the crack growth under time-varying load condition. The proposed method first extracts damage indexes from the collected signals to construct the baseline model as well as the online FCM model. Migration index of the online model is calculated by Kullback-Liebler Divergence (KLD) and Bhattacharyya Distance (BD), respectively. By comparing with the Gaussian mixture model (GMM), experimental results show that the proposed FCM algorithm has less computation time and its migration index curve is smoother when the crack size is small. Furthermore, KLD achieves a higher sensitivity than BD as crack grows.

INDEX TERMS Crack monitoring, time-varying load, FCM clustering algorithm, KLD migration index.

I. INTRODUCTION

Lamb wave is considered to be one of the most promising structural health monitoring techniques for online and real-time damage monitoring of aircraft structures due to its ability to travel long distance and monitor large area [1]. The traditional Lamb wave signal processing methods usually first extract the signal features such as time of flight, amplitude, energy, and correlation coefficient with the reference signal to construct the damage index (DI), and the damage imaging technology is applied to further show the damage information intuitively [2]–[8]. These methods assume that the environmental conditions stay unchanged. However, the aircraft usually works under time-varying environment, by which the above features of the Lamb wave will be directly and significantly affected. It is difficult to obtain accurate damage information by using traditional damage detection methods when considering environmental factors. Thus, an effective damage identifying technology needs to be developed to solve this problem.

Damage monitoring technologies based on probability and statistical model have achieved wide concentration in recent years. The Gaussian mixture model (GMM) was first applied by Banerjee *et al.* [9] for hot spot monitoring to minimize the damage estimation error. They proved that it can effectively predict the crack extent though the temperature of the specimen increased in the last loading cycle. Qiu *et al.* [10] proposed an online updating damage monitoring method based on the GMM. They first collected a set of baseline signals under time-varying conditions to build a baseline model, and compared the online model and the baseline model by Kullback-Leibler divergence (KLD). They further optimized the GMM to improve the performance of the GMM-based damage monitoring method under time-varying conditions [11]–[13]. Anaya *et al.* [14] presented a structural state classification method based on statistical data-driven model combining multi-path principal component analysis (MPCA), discrete wavelet transform (DWT) and self-organizing map (SOM). It was demonstrated that in the aluminum plate and the reinforced composite plate, the proposed model was able to distinguish not only the healthy state and the damage state of the structure but also the damage state of the piezoelectric sheet when the

The associate editor coordinating the review of this article and approving it for publication was Noor Zaman.

temperature changed. Chakrabort *et al.* [15] utilized the Dirichlet Process (DP) mixture model combining the physical damage model to estimate damage state under the influence of time-varying conditions.

Besides all the above technologies, Fuzzy c-means (FCM) algorithm has also achieved concentration of researchers due to its short running time and high accuracy. Chen *et al.* [16] used the circular and parallel linear piezoelectric array to verify the feasibility of FCM algorithm to identify single damage and two damages in the plate. Results shows that the positioning errors in both situations were less than 3mm. Jac Fredo *et al.* [17] demonstrated the ability of the FCM algorithm to classify local and global damage in the composite panel. Zeng *et al.* [18] combined the time series model with the FCM algorithm to determine whether the structure was damaged or not, and verified the effectiveness of this method on estimating the damage severity of the bridge. The above studies with regard to the FCM algorithm show that the FCM algorithm has an excellent ability in damage identification.

Both GMM and FCM are soft-clustering algorithms. GMM performs well in clustering, but its running speed is often longer due to the calculation of Gaussian Distribution, especially when the chosen number of clusters is large. FCM is widely used for its performance and speed. It provides a degree of membership for each sample, which is very useful when we are not certain about the observed objects [19]. Therefore, in this paper FCM algorithm is tried to apply on the crack growth monitoring under the time-varying load condition. A baseline model and the real-time model are established by FCM algorithm respectively. The efficiency of the proposed method is demonstrated by comparing the proposed method with the GMM technology. In addition, two migration indexes, Kullback-Liebler Divergence (KLD) [20] and Bhattacharyya Distance (BD) [21], describing the migration degree between the baseline model and the online model are compared in this paper.

The paper is organized as follows: Section II introduces the principle of the FCM algorithm to monitor crack growth for hot-spot structures. In Section III, experiments were conducted to verify the feasibility of the proposed FCM model to track crack growth under the time-varying load condition, and a comparison with the GMM was made in Section III as well. Finally, conclusions are drawn in Section IV.

II. PRINCIPLES OF FCM ALGORITM TO MONITOR CRACK GROWTH

A. FCM ALGORITHM

In the traditional set theory, the feature that judges whether a variable belongs to a certain set is 0 or 1. However, the process is more complicated in the fuzzy set theory with a membership degree between 0 and 1 for each variable instead of only 0 or 1. It is subject to the principle that one point belongs to multiple clusters. Therefore, the fuzzy set theory often achieves a good performance for characterizing uncertainties.

Assuming that the damage index (DI) extracted from the Lamb wave signal under the time-varying condition is $X = \{x_1, \ldots, x_r, \ldots, x_n\}$, where n represents the number of collected signals in a feature space, x_r is a d-dimensional feature vector consisting of d *DI*s chosen as the input of the algorithm. There are c cluster centers if the data are divided into c fuzzy sets. The membership degree of jth sample to the ith cluster is represented as u_{ij}, which denotes the similarity between the sample j and the certain cluster i. A crucial point of the FCM clustering algorithm is to find an appropriate membership degree to minimize the objective function as follows

$$J = \sum_{i=1}^{c}\sum_{j=1}^{n} u_{ij}^{m} \left\| x_j - c_i \right\|^2 \tag{1}$$

$$\sum_{i=1}^{C} u_{ij} = 1 \tag{2}$$

where $\left\| x_j - c_i \right\|^2$ is the distance from the sample j to the cluster center i, and m is the weighting fuzziness parameter. u_{ij} is constrained by (2). By solving $\partial J/\partial u_{ij} = 0$ and $\partial J/\partial c_i = 0$ based on Lagrange Multiplier Method, the iterative formulas of u_{ij} and c_i can be expressed as

$$u_{ij} = \frac{1}{\sum_{k=1}^{c}\left(\frac{\|x_j - c_i\|}{\|x_j - c_k\|}\right)^{\left(\frac{2}{m-1}\right)}} \tag{3}$$

$$c_i = \frac{\sum_{j=1}^{n}\left(x_j u_{ij}^{m}\right)}{\sum_{j=1}^{n} u_{ij}^{m}} \tag{4}$$

Therefore, the iterative process of the FCM algorithm can be concluded as follows:

Step 1: Set the initial number of clusters (c), the weighting fuzziness parameter (m), the threshold (ε), the maximum number of iterations (L) and the initial the membership value (u_{ij}).

Step 2: Calculate the cluster center c_i according to (1)-(4).

Step 3: Calculate the value of the objective function. If the change of the objective function value is greater than the set threshold, update u_{ij} and return to step 2. On the contrary, if it is less than the set threshold or the iterations reaches the maximum number L, the iteration ends. The parameters obtained by the FCM algorithm can effectively describe the distribution of the data set.

B. CRACK DETECTION PROCESS BASED ON THE FCM ONLINE MODEL

The main process of the crack monitoring model proposed in this paper is shown in Figure 1. First, a set of baseline signals in a healthy plate before the crack appears are collected to establish a baseline model through the FCM algorithm.

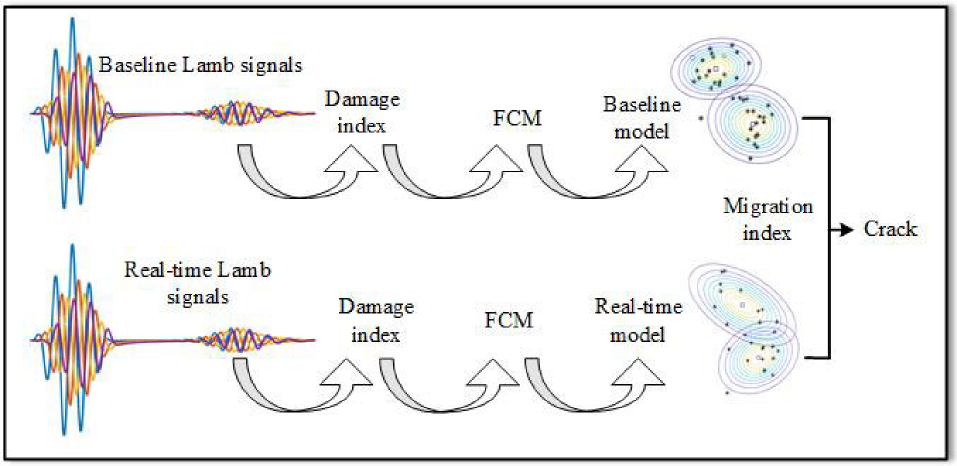

FIGURE 1. Process of crack monitoring based on the FCM algorithm.

Second, when the crack propagates under time-varying load conditions, real-time Lamb wave signals are used to build the online model. Finally, the online model is compared with the baseline model by calculating the migration index between them, which is used to indicate the condition of crack growth.

According to the FCM algorithm, two *DI*s are selected here to form the feature vectorx_r. The first *DI* is

$$DI_1 = \sqrt{\frac{\int_{w_o}^{w_1} (|b(w)| - |m(w)|)^2 dw}{\int_{w_o}^{w_1} (|b(w)|)^2 dw}} \tag{5}$$

where $b(w) = \int_{t_0}^{t_1} b(t)e^{-jwt}dt$, $m(w) = \int_{t_0}^{t_1} m(t)e^{-jwt}dt$, $b(t)$ and $m(t)$ are the reference signal and the online signal, respectively. w_0 and w_1 are the start and the end frequencies of the selected spectrum, respectively. The second *DI*is

$$DI_2 = \sqrt{\frac{\int_{t_0}^{t_1} (m(t) - b(t))^2 dt}{\int_{t_0}^{t_1} b^2(t)dt}} \tag{6}$$

where t_0 and t_1 represent the start and the end time of the selected wave packet, respectively. Therefore, the $x_r = [DI_1, DI_2]^T$. The baseline data set and every online model consists of consecutive 120 signals in this paper. Two migration indexes, *KLD* and *BD*, are applied respectively in this paper to quantify the migration between the baseline model φ (0) and the *n*th online model φ (*n*). The calculation equation of the *KLD* is

$$\begin{aligned} &KLD\left(\varphi_i(0), \varphi_j(n)\right) \\ &= \frac{1}{2}\left\{tr\left((\Sigma_j^n)^{-1}\Sigma_i^0\right) + \left(\mu_j^n - \mu_i^0\right)^T (\Sigma_j^n)^{-1}\left(\mu_j^n - \mu_i^0\right) \right. \\ &\quad \left. - d + \ln\frac{\left|\Sigma_j^n\right|}{\left|\Sigma_i^0\right|}\right\} \end{aligned} \tag{7}$$

The calculation equation of the *BD* is

$$\begin{aligned} BD\left(\varphi_i(0), \varphi_j(n)\right) &= \frac{1}{8}\left(\mu_j^n - \mu_i^0\right)^T \left[\frac{\Sigma_i^0 + \Sigma_j^n}{2}\right]^{-1} \\ &\quad \times \left(\mu_j^n - \mu_i^0\right) + \frac{1}{2}\ln\frac{\left|\frac{\Sigma_i^0 + \Sigma_j^n}{2}\right|}{\sqrt{\left|\Sigma_i^0\right|\left|\Sigma_j^n\right|}} \end{aligned} \tag{8}$$

where $\varphi_j(n)$ denotes the *j*th component of the *n*th FCM model. Σ_j^n and μ_j^n are the covariance matrix and the mean vector for component $\varphi_j(n)$, and of the baseline model when $n = 0$. $|\bullet|$ represents the determinant and d is the dimension of the feature vector x_r. Then the migration index between $\varphi(0)$ and $\varphi(n)$ for both *KLD* and *BD* is further defined as[22]

$$MI(\varphi(0), \varphi(n)) = \sum_{i=1}^{c} w_i \min_j \left\{D(\varphi_i(0), \varphi_j(n)) + \ln\frac{w_i}{w_j}\right\} \tag{9}$$

where *D* represents *KLD* or *BD*. The relationship between the crack length and the migration index can be established by calculating the migration index of the reference model and the online model.

III. EXPERIMENT

According to the relevant test standard for fatigue crack growth rate of metallic materials, the test specimen was customized for the experiment as shown in Figure 2. The specimen with dimensions $125mm \times 120mm \times 6mm$ was made of T-6061 aluminum alloy with tensile strength of 290Mpa and yield strength of 240Mpa. There was a cut with 42mm in length and 6mm in width in the middle of the specimen. A prefabricated crack ($1mm \times 1mm \times 6mm$) was obtained by wire cutting at the end of the cut. Two piezoelectric sensors with an interval of 10cm were arranged 10mm from the cut on the specimen. Figure 3 shows the experimental setup. The fatigue machine (WEW-100B) with a maximum load of 6kN was used to apply sinusoidal alternating load with a frequency

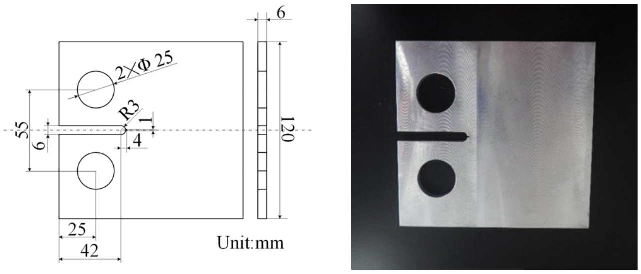

FIGURE 2. The specimen in the experiment.

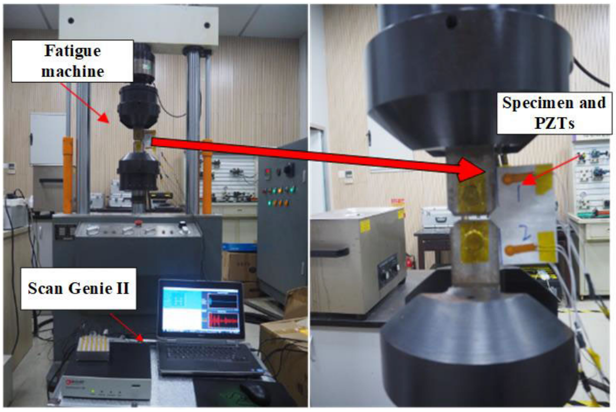

FIGURE 3. Experimental setup.

of 10Hz. ScanGenie II made by Acellent technologies was used for signal generation and acquisition. In the experiment, fatigue machine would stop at intervals and keep the load at the current load value to measure the crack length and acquire the Lamb wave signals.

A five-circle sinusoidal tone burst, modulated by a Hanning window, with a central frequency of 100kHz was used as the exciting signal. The sampling rate was 12M/s and the number of sampling points was 6000. A total of 200 groups of signals numbered from Signal No.1 to Signal No.200 were collected in the experiment. According to the group velocity of the Lamb wave and the sensor distance, it can be known that the S0 wave arrives roughly between 50 microseconds and 100 microseconds. Figure 4 shows S0 wave packets of the Signal Nos.7-9. Since the signals were collected continuously, the crack growth can be almost ignored during such a short time. It can be observed from the signals that the load has an obvious effect on the amplitude and flight time of the Lamb wave signal.

In the FCM model, Signal No.1 is the baseline signal mainly applied to calculate the *DI*s of the rest 199 signals. First, two *DI*s of each signal are calculated by (5) and (6), respectively, and their variation trends are shown in Figure 5. It can be observed that it is difficult to directly find an effective trend of both *DI*s as the crack grows under the time-varying load, especially in the early period of the crack growth. Second, two *DI*s are utilized to establish the FCM model at every stage during the process of crack growth, which are compared to the results of the GMM [10]. Some parameters of the FCM model are as follows: $c = 2$,

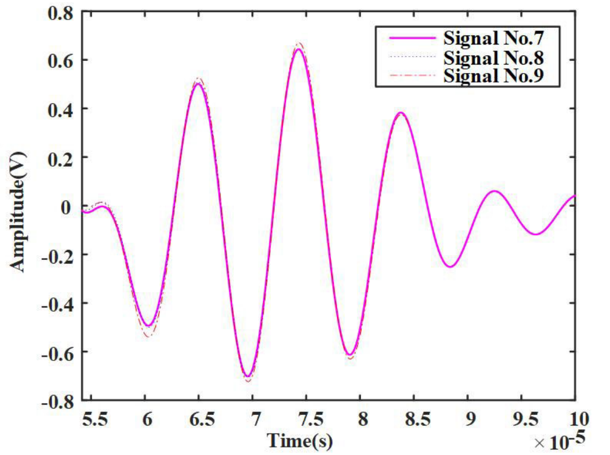

FIGURE 4. S0 wave packets of the Signals Nos.7–9.

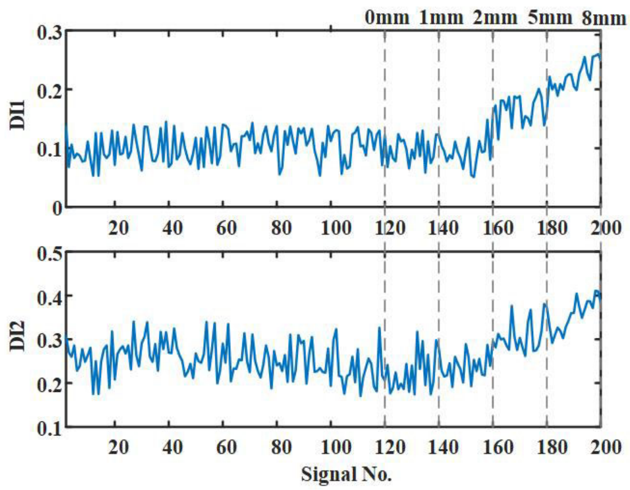

FIGURE 5. Variation of two *DI*s.

$m = 2$, $L = 100$, $\varepsilon = 10^{-10}$. The threshold set for GMM is also 10^{-10}. For both FCM and GMM, the other initial parameters of the baseline model are set by K-means algorithm and the results of the (k)th model are served as the initial value of the $(k+1)$th model to minimize the impact of initial value on the clustering results.

The influence of two factors, including the number n of signals in the feature space and the number c of clusters, on the clustering results is analyzed and shown in Figures 6-9. The number of signals applied in each model was first considered. Conclusions of Figure 6 and Figure 7 can be drawn as follows: 1) When 120 signals were applied in each model, two migration indexes of both FCM and GMM models achieve a relatively stable upward trend with the growth of the crack, which can be attributed to the fact that when the sample size is larger, the trend of data is more obvious; 2) By comparing the trend of *KLD* and *BD*, it can be observed that the value of *KLD* changes much more than the value of *BD* as crack grows. Thus, 120 signals were applied to construct a model for both FCM and GMM algorithm when considering the effect of the number of clusters on the results, which are

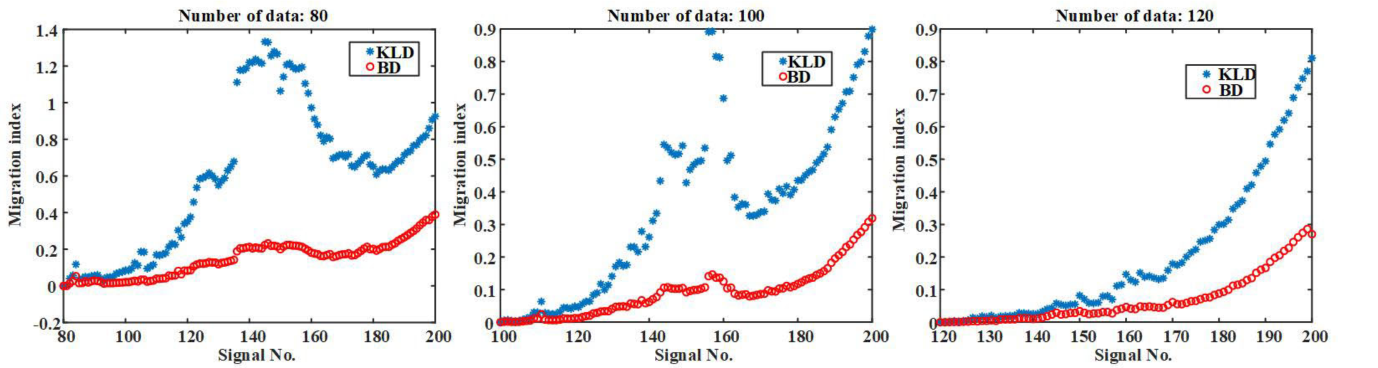

FIGURE 6. Migration index of FCM model versus number of data.

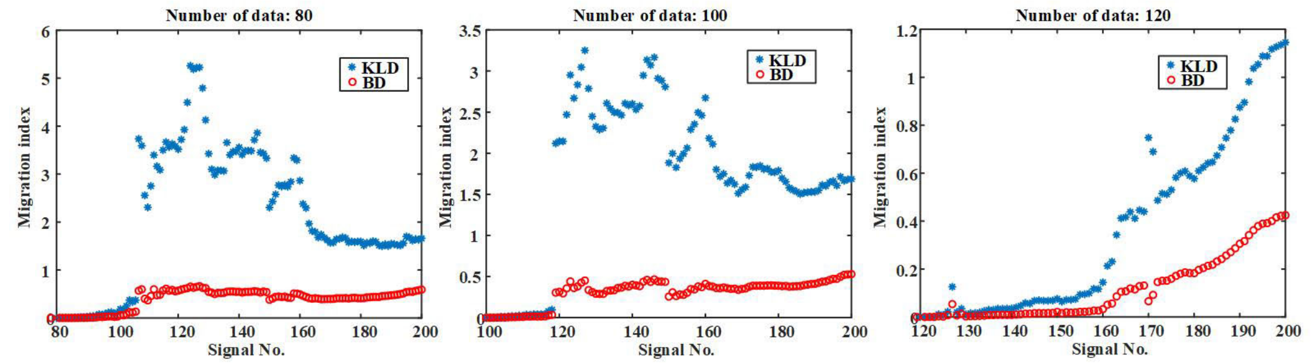

FIGURE 7. Migration index of GMM versus number of data.

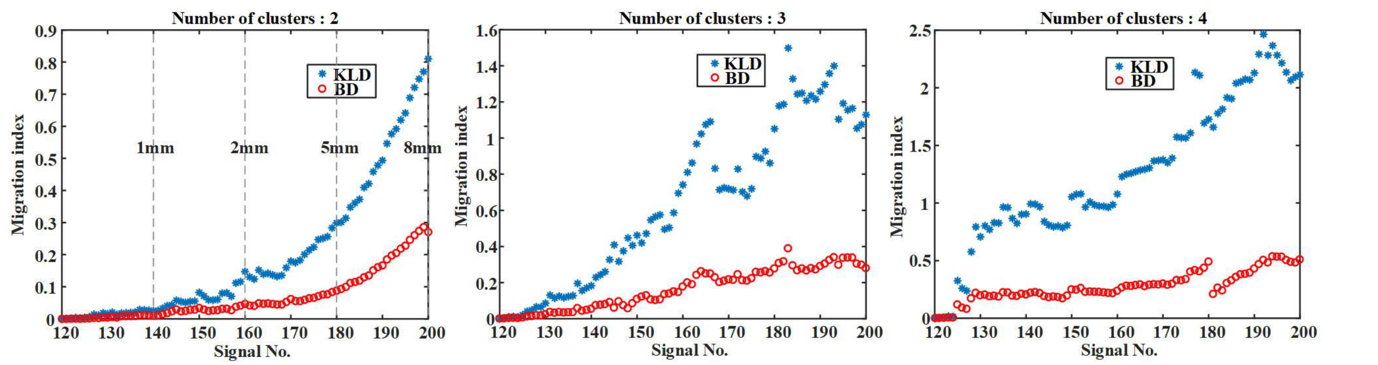

FIGURE 8. Migration index of FCM model versus number of clusters.

shown in Figures 8 and 9. It is obvious that when the number of clusters is 2, the migration index has a best ability of characterizing the crack growth. When the number of clusters increases, the migration index shows an upward trend, but its linearity decreases.

In summary, 120 signals are used and divided into 2 stages for both FCM and GMM models. When the crack is 0mm, 1mm and 8 mm, more concrete clustering results of the FCM and the GMM are presented in Figures 10 and 11, respectively. Comparison between the FCM model and the GMM can be concluded as followings: 1) It is hard for both FCM and GMM to identify the crack under 1mm, which is related to the central frequency of Lamb wave; 2) For both algorithms, the change of *KLD* is much bigger than *BD* as crack grows; 3) The FCM algorithm can be used to estimate the growth of crack under time-varying load; 4) The migration index of the FCM model changes smaller than that of the GMM, but it can be seen from the migration index curve that when the crack size is as small as 2-5mm, FCM has a better smoothness than GMM; 5) The running time of the FCM algorithm(1.234s) is shorter than that of the GMM algorithm(2.487s), and the calculation time is vital and influences the real-time nature of monitoring when there are plenty of hots-pots. As a result, FCM algorithm offers an alternative method for crack monitoring with a better performance and fewer running time.

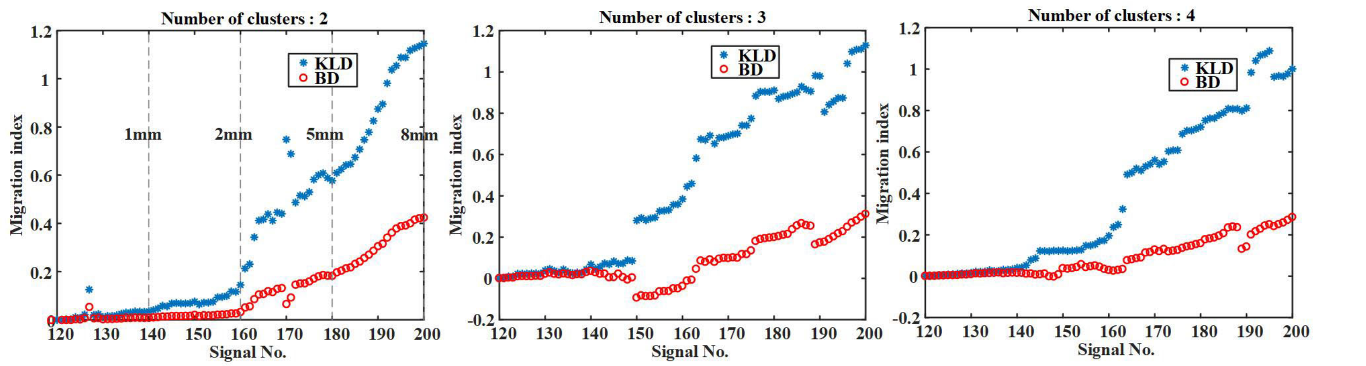

FIGURE 9. Migration index of GMM model versus number of clusters.

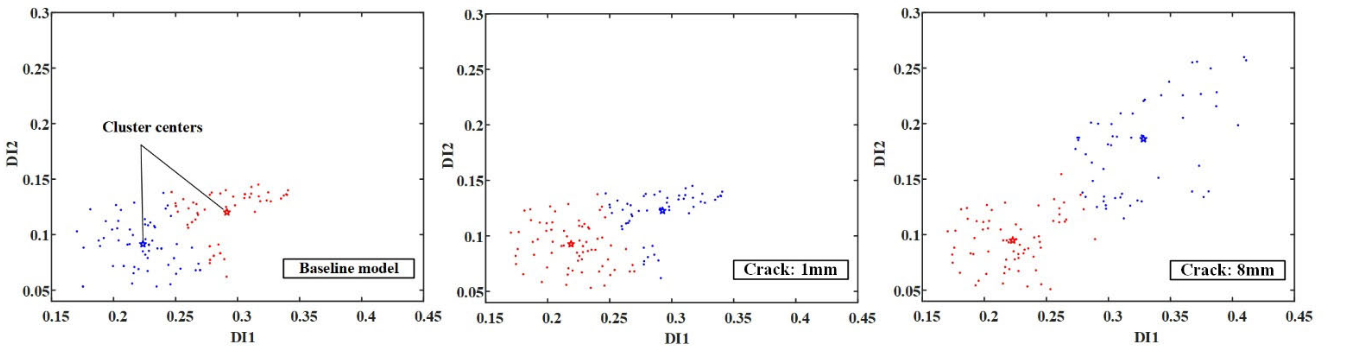

FIGURE 10. Baseline model and online models of the FCM.

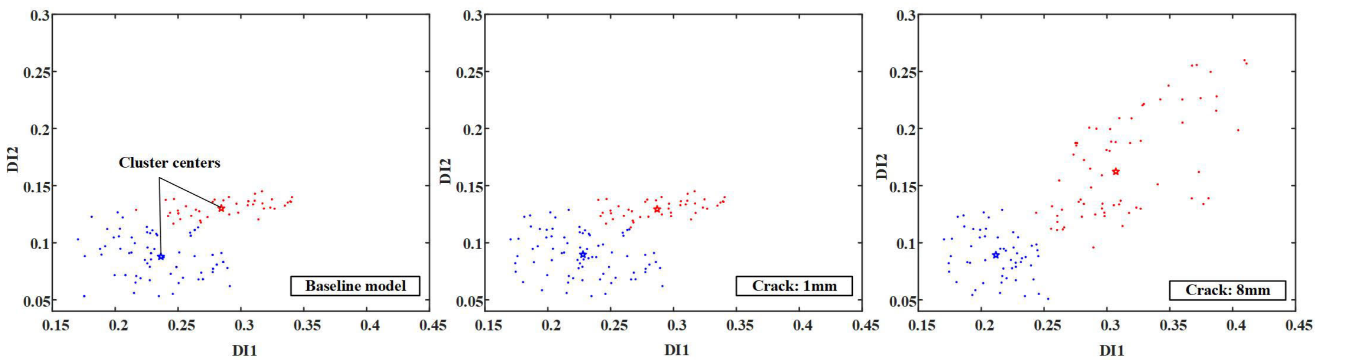

FIGURE 11. Baseline model and online models of the GMM.

IV. CONCLUSION

In this paper, crack growth monitoring technology based on the FCM algorithm is proposed for hot-spot structures under time-varying load conditions. Based on the experiment verification, it is clear that the proposed method can eliminate the effect of load on the Lamb wave and monitor the crack growth. The following remarks can be made on the investigation:

1) When the crack length is larger than 1mm, the proposed FCM algorithm can obviously monitor the crack growth although it is difficult to view the increasement of *DI*.
2) Two type of migration indexes named *KLD*and *BD* are developed to calculate the migration degree of two FCM models. The result shows that *KLD* is more sensitive to the crack growth than *BD*.
3) The relationship between migration index and the crack length depends on not only the location of sensors but also the geometry and the material of structural pieces. Thus, the relationship must be calibrated by one piece at least by experiment, which can be used for other pieces.

ACKNOWLEDGMENT

The authors acknowledge the support of Xiamen Key laboratory of Optoelectronic Transducer Technology and Fujian Key Laboratory of Universities & Colleges for Transducer Technology.

REFERENCES

[1] X. Qing, W. Li, Y. Wang, and H. Sun, "Piezoelectric transducer-based structural health monitoring for aircraft applications," *Sensors*, vol. 19, no. 3, pp. 545–571, Jan. 2019.

[2] Y. Wang, R. Guan, and Y. Lu, "Nonlinear Lamb waves for fatigue damage identification in FRP-reinforced steel plates," *Ultrasonics*, vol. 80, pp. 87–95, Sep. 2017.

[3] T. R. Hay, R. L. Royer, H. Gao, X. Zhao, and J. L. Rose, "A comparison of embedded sensor Lamb wave ultrasonic tomography approaches for material loss detection," *Smart Mater. Struct.*, vol. 15, no. 4, pp. 946–951, Jun. 2006.

[4] L. Zhou, H. Sun, and Z. He, "Fractal dimension-based damage imaging for composites," *Shock Vib.*, vol. 20, no. 5, pp. 979–988, Apr. 2013.

[5] A. Ebrahimkhanlou, B. Dubuc, and S. Salamone, "Damage localization in metallic plate structures using edge-reflected Lamb waves," *Smart Mater. Struct.*, vol. 25, no. 8, Jul. 2016, Art. no. 085035.

[6] Y. Liu, S. Zhou, H. Ning, C. Yan, and N. Hu, "An inverse approach of damage identification using Lamb wave tomography," *Sensors*, vol. 19, no. 9, pp. 2180–2193, May 2019.

[7] H. Sun, A. Zhang, Y. Wang, and X. Qing, "Baseline-free damage imaging for metal and composite plate-type structures based on similar paths," *Int. J. Distrib. Sensor Netw.*, vol. 15, no. 4, pp. 1–14, 2019.

[8] Z. Liu, X. Zhong, T. Dong, C. He, and B. Wu, "Delamination detection in composite plates by synthesizing time-reversed Lamb waves and a modified damage imaging algorithm based on RAPID," *Struct. Control Health Monit.*, vol. 24, no. 5, p. e1919, Jul. 2017.

[9] S. Banerjee, X. P. Qing, S. Beard, and F.-K. Chang, "Prediction of progressive damage state at the hot spots using statistical estimation," *J. Intell. Mater. Syst. Struct.*, vol. 21, no. 6, pp. 595–605, Apr. 2010.

[10] L. Qiu, S. Yuan, F.-K. Chang, Q. Bao, and H. Mei, "On-line updating Gaussian mixture model for aircraft wing spar damage evaluation under time-varying boundary condition," *Smart Mater. Struct.*, vol. 23, no. 12, pp. 125001–125014, Oct. 2014.

[11] L. Qiu, S. Yuan, H. Mei, and F. Fang, "An improved Gaussian mixture model for damage propagation monitoring of an aircraft wing spar under changing structural boundary conditions," *Sensors*, vol. 16, no. 3, pp. 291–308, Feb. 2016.

[12] L. Qiu, F. Fang, S. Yuan, C. Boller, and Y. Ren, "An enhanced dynamic Gaussian mixture model–based damage monitoring method of aircraft structures under environmental and operational conditions," *Struct. Health Monit.*, vol. 18, no. 2, pp. 524–545, 2018.

[13] L. Qiu, F. Fang, and S. Yuan, "Improved density peak clustering-based adaptive Gaussian mixture model for damage monitoring in aircraft structures under time-varying conditions," *Mech. Syst. Signal Process.*, vol. 126, pp. 281–304, Jul. 2019.

[14] M. Anaya, D. A. Tibaduiza, M. A. Torres-Arredondo, F. Pozo, M. Ruiz, L. E. Mujica, J. Rodellar, and C.-P. Fritzen, "Data-driven methodology to detect and classify structural changes under temperature variations," *Smart Mater. Struct.*, vol. 23, no. 4, Feb. 2014, Art. no. 045006.

[15] D. Chakraborty, N. Kovvali, A. Papandreou-Suppappola, and A. Chattopadhyay, "An adaptive learning damage estimation method for structural health monitoring," *J. Intell. Mater. Syst. Struct.*, vol. 26, no. 2, pp. 125–143, 2014.

[16] S. Chen, S. Zhou, C. Chen, Y. Li, and S. Zhai, "Detection of double defects for plate-like structures based on a fuzzy C-means clustering algorithm," *Struct. Health Monit.*, vol. 18, no. 3, pp. 757–766, 2018.

[17] A. R. J. Fredo, R. S. Abilash, R. Femi, A. Mythili, and C. S. Kumar, "Classification of damages in composite images using Zernike moments and support vector machines," *Compos. B, Eng.*, vol. 168, pp. 77–86, Jul. 2019.

[18] Y. Zeng, Y. Yan, S. Weng, Y. Sun, W. Tian, and H. Yu, "Fuzzy clustering of time-series model to damage identification of structures," *Adv. Struct. Eng.*, vol. 22, no. 4, pp. 868–881, 2018.

[19] Y. Hu, L. Wai, and S. Chee, "Clustering algorithms for scene classification—A performance comparison between K-means; fuzzyc-means and GMM," in *Proc. IIEEJ Image Electron. Vis. Comput. Workshop*, Kuching, Malaysia, Nov. 2012, pp. 1–6.

[20] J. Goldberger, S. Gordon, and H. Greenspan, "An efficient image similarity measure based on approximations of KL-divergence between two Gaussian mixtures," in *Proc. 9th IEEE Int. Conf. Comput. Vis.*, Oct. 2003, pp. 487–493.

[21] A. Gupta and D. Kumar, "Fuzzy clustering-based feature extraction method for mental task classification," *Brain Inform.*, vol. 4, pp. 135–145, Jun. 2016.

[22] R. Li, N. Jan, B. Huang, and V. Prasad, "Constrained multimodal ensemble Kalman filter based on Kullback–Leibler (KL) divergence," *J. Process Control*, vol. 79, pp. 16–28, Jul. 2019.

HU SUN received the B.S. degree in aircraft design and engineering and the Ph.D. degree in engineering mechanics from the Nanjing University of Aeronautics and Astronautics, China, in 2007 and 2014, respectively.

He is currently an Assistant Professor with Xiamen University. His current research interests include structural health monitoring, advanced sensing technology, and advanced NDT technology.

JUNYAN YI received the B.S. degree in measurement and control technology and instrumentation from China Jiliang University, in 2018. She is currently pursuing the M.S. degree in measurement technology and instrument with Xiamen University.

Her current research interests include structural health monitoring and advanced sensing technology.

YU XU received the B.S. degree in measurement and control technology and instrumentation from Nanchang Hangkong University, in 2015, and the M.S. degree in mechanical engineering from Xiamen University, in 2018.

His current research interest includes anomaly detection algorithm.

YISHOU WANG received the B.S. degree in mechanical design and automation and the Ph.D. degree in mechanical engineering from the Dalian University of Technology, China, in 2002 and 2008, respectively.

He is currently an Associate Professor with Xiamen University. His current research interests include aircraft health management and structural health monitoring.

XINLIN QING received the M.S. degree in experimental mechanics from Tianjin University, in 1991, and the Ph.D. degree in solid mechanics from Tsinghua University, in 1993.

He is currently a Distinguished Professor with Xiamen University. His current research interests include aircraft health management, structural health monitoring, advanced sensing technology, intelligent structure, and composites and its repair technology.